# Dipyrenylphosphatidylcholines as membrane fluidity probes

## Pressure and temperature dependence of the intramolecular excimer formation rate

Massimo Sassaroli,* Matti Vauhkonen,‡ Pentti Somerharju,‡ and Suzanne Scarlata§

*Department of Physiology and Biophysics, Mount Sinai School of Medicine, New York, New York 10029-6574 USA; ‡Department of Medical Chemistry, Faculty of Medicine, University of Helsinki, 00170 Helsinki, Finland; and §Department of Physiology and Biophysics, State University of New York Health Sciences Center at Stony Brook, Stony Brook, New York 11794-8661 USA

ABSTRACT We have measured the pressure dependence of the intramolecular excimer formation rate, K(p), for di-(1′-pyrenedecanoyl)-phosphatidylcholine ($dipy_{10}PC$) probes in single-component lipid multilamellar vesicles (MLV) as a function of temperature. Apparent volumes of activation ($V_a$) for intramolecular excimer formation are obtained from the slopes of plots of log K(p) versus P. For liquid-crystalline saturated lipid MLV (DMPC and DPPC), these plots are linear and yield a unique $V_a$ at each temperature, whereas for unsaturated lipids (POPC and DOPC) they are curvilinear and $V_a$ appears to decrease with pressure. The isothermal pressure induced phase transition is marked by an abrupt drop in the values of K(p). The pressure to temperature equivalence values, $dP_m/dT$, estimated from the midpoint of the transitions, are 47.0, 43.5, and 52.5 bar $°C^{-1}$ for DMPC, DPPC, and POPC, respectively.

In liquid-crystalline DMPC, $V_a$ decreases linearly as a function of temperature, with a coefficient $-dV_a/dT = 0.65 \pm 0.11$ ml $°C^{-1}$ $mol^{-1}$. Using a modified free volume model of diffusion, we show that this value corresponds to the thermal expansivity of DMPC.

Both the apparent energy and entropy of activation, $E_a$ and $\Delta S_a$, increase with pressure in DMPC, whereas both decrease in POPC and DOPC. This difference is attributed to the sensitivity of the dynamics and/or packing of the $dipy_{10}PC$ probes to the location of the *cis*-double bonds in the chains of the unsaturated host phospholipids.

Finally, the atmospheric pressure values of $E_a$ and $\Delta S_a$ for the four host MLV examined are shown to be linearly related. The relevance of this finding with respect to the structure of the excimers formed by the $dipy_{10}PC$ probes is briefly discussed.

## INTRODUCTION

A variety of experimental tools have been applied to characterize the dynamic and structural properties of biological and model lipid membranes. In particular, because of their great sensitivity and versatility, fluorescence and fluorescent lipid analogues have found use in many methodologies, such as in fluorescence recovery after photobleaching measurements of long-range lateral diffusion (Wu et al., 1977; Vaz et al., 1982), in measurements of short-range lateral diffusion by the intermolecular excimer technique (Galla et al., 1979; Eisinger et al., 1986; Hresko et al., 1986; Sassaroli et al., 1990), and in fluorescence polarization measurements of probe rotational mobility and of lipid packing fluctuations (Andrich and Vanderkooi, 1977; Dale et al., 1977; Davenport et al., 1989).

Pyrene and its derivatives have long been known to undergo an excited state reaction in which two molecules, one in the excited state and the other in the ground state, form an excited state dimer, or excimer, whose fluorescence is substantially red-shifted with respect to that of the monomer (Förster and Kasper, 1955; Birks, 1970). For the case of monopyrenyl phosphatidylcholine analogues ($py_nPC$), in which one of the phospholipid chains is $n$-carbon long and its terminal methyl is reacted with a pyrene moiety, the probability of excimer formation is determined by the concentration of the probes and their lateral diffusivity. In general, probe/lipid mole fractions of the order of a few percent need to be used to obtain an appreciable excimer fluorescence signal.

Dipyrenylphosphatidylcholines ($dipy_nPC$) are phospholipid derivatives in which one pyrene moiety is conjugated to the terminal methyl of each of the two $n$-carbon long acyl chains. When these probes are inserted in a host membrane at a probe/lipid mole fraction $x \approx 0.001$, the probability of excimer formation is concentration independent and is related to the motional freedom of the two pyrene moieties limited by the configuration of the acyl chains to which they are attached and the packing of the surrounding phospholipid environment. The greatest advantage of the $dipy_nPC$ probes over their monopyrenyl analogues is that they can be used at very low concentration, which results in minimal perturbation of the host lipid membrane and eliminates any artifacts from probe segregation that may occur at the higher concentrations required by the intermolecular probes.

The sensitivity of di-(1′-pyrenedecanoyl)-phosphatidylcholine ($dipy_{10}PC$) probes to the physicochemical properties of lipid membranes, such as their phase state, was demonstrated in a previous study of the temperature dependence of the intramolecular excimer formation rate in a variety of model lipid membranes (Vauhkonen et al., 1990). In that article, it was also shown that a linear relationship exists between the intramolecular excimer formation rate for $dipy_{10}PC$ probes and the intermolecular excimer formation rate for 1-palmitoyl-2-(1′-pyrenedecanoyl)-PC ($py_{10}PC$) probes, which has been used to measure translational diffusion in artificial and natural membrane systems. It was therefore suggested that both processes may be rate limited by the same step, possibly the rotation of the pyrene moieties.

In the present study, we use hydrostatic pressure as an additional thermodynamic variable to investigate in more detail the behavior of these probes in well charac-


0006-3495/93/01/137/13 $2.00

terized homogeneous phosphatidylcholine host membranes and to gain a deeper insight into the microscopic properties of the lipid environment surrounding these fluidity probes.

## EXPERIMENTAL METHODS

The phospholipids 1,2-dimyristoyl-*sn*-glycero-3-phosphatidylcholine (DMPC), 1,2-dipalmitoyl-*sn*-glycero-3-phosphatidylcholine (DPPC), 1-palmitoyl-2-oleoyl-*sn*-glycero-3-phosphatidylcholine (POPC), and 1,2-dioleoyl-*sn*-glycero-3-phosphatidylcholine (DOPC) were obtained from Avanti Polar Lipids (Alabaster, AL) and were used without further purification. The lipids were dissolved at a concentration of ~10 mM in an organic solvent mixture (CM, chloroform/methanol, 4:1 by volume) and were stored at −20°C; their concentrations were determined by use of a phosphate assay (Bartlett, 1959). $Py_{10}PC$ was obtained from Molecular Probes, Inc. (Eugene, OR). $Dipy_{10}PC$ was synthesized by methods described previously (Patel et al., 1979). The monopyrenyl and dipyrenyl probes were dissolved in the CM solvent at a concentration of ~100 μM, and their concentrations were determined spectrophotometrically, using 42,000 $cm^{-1}$ as the molar extinction coefficient of pyrene at 342 nm in ethanol.

Pyrenyl probes were added to the phospholipids at a molar ratio of 0.1% in the CM solvent; the mixture was then dried under a stream of nitrogen gas and placed under vacuum for 15 h to eliminate any residual solvent. Multilamellar vesicles (MLV) at a lipid concentration of 0.1 mM were prepared by adding buffer (10 mM *N*-2-hydroxyethylpiperazine-*N'*-2-ethane sulfonic acid, pH 7.2, 5 mM KCl, 140 mM NaCl) to the dry lipids and vortexing intermittently; during hydration, the temperature of the sample was maintained well above the gel–liquid-crystalline phase transition temperature of the matrix lipids. Finally, the lipid suspensions were sonicated for 15 min in a low-power ultrasonic bath (model 2200; Branson Inc., Danbury, CT).

Fluorescence intensity measurements under pressures ranging from 1 bar to 2 kbar were performed by means of a thermostatted pressure vessel based on a previously described design (Paladini and Weber, 1981) fitted in the sample compartment of an ISS GREG-PC (ISS, Champaign, IL). Pressure increments of 50 or 100 bar were used, and the samples were allowed to equilibrate for several minutes before measuring the fluorescence intensities. Reversibility was confirmed by repeating some measurements during depressurization; these intensity and ratio values were within 5% of those measured during the pressurization cycle. The excitation light at 325 nm was provided by either a He-Cd laser (Liconix, Sunnyvale, CA) or an Xe-arc lamp, and the monomeric and excimeric emissions were measured at 380 and 480 nm, respectively. Samples were not deoxygenated.

## DATA ANALYSIS

The following analysis is an extension of that previously developed to derive a relationship between the intramolecular excimer formation rate, $K$, for $dipy_{10}PC$ probes and the concentration dependent intermolecular excimer formation rate, $K(x)$, for $py_{10}PC$ probes (Vauhkonen et al., 1990). One important but reasonable assumption of this model is that the pyrene monomer and excimer radiative and nonradiative rate constants depend exclusively on the properties of the surrounding medium and are the same for monopyrenyl and dipyrenyl-PC probes dissolved in similar lipid environments.

The kinetic scheme for an intramolecular excimeric probe is summarized below

$$M + M^* \xrightarrow{K} (MM)^*$$

$$M^* \xrightarrow{k_M, k'_M} M + h\nu_M$$

$$(MM)^* \xrightarrow{k_E, k'_E} 2M + h\nu_E,$$

where $M$ and $M^*$ represent the ground and excited state monomeric pyrene, $(MM)^*$ represents the excited state dimer or excimer, $k$ and $k'$ are the radiative and nonradiative decay rates with subscripts M and E denoting photon emission ($h\nu$) from excited monomers and excimers, respectively. In the temperature range of our investigations, the rate of excimer dissociation is small compared with $(k_E + k'_E)$ and, therefore, it has been omitted from the kinetic scheme (Galla and Sackmann, 1974; Zachariasse et al., 1980).

The $dipy_{10}PC$ monomer and excimer fluorescence quantum yields, $\phi_M$ and $\phi_E$, are then given by

$$\phi_M = \frac{k_M}{k_M + k'_M + K} \tag{1}$$

$$\phi_E = \frac{k_E}{(k_E + k'_E)} \frac{K}{(k_M + k'_M + K)}. \tag{2}$$

A similar kinetic scheme can be used to describe the process of intermolecular excimer formation by $py_{10}PC$, with the exception that the intermolecular excimer formation rate, $K(x)$, depends on the mole fraction of the probes, $x$, as well as on their translational mobility (Sassaroli et al., 1990). If $py_{10}PC$ probes are dispersed at a concentration sufficiently low to preclude excimer formation in vesicles composed of the same phospholipids as those in which $dipy_{10}PC$ is dissolved, the intermolecular excimer formation rate $K(x) = 0$ and the intrinsic monomer fluorescence quantum yield is given by

$$\phi^*_M = \frac{k_M}{k_M + k'_M}. \tag{3}$$

On the other hand, if the mole fraction of $py_{10}PC$ is so high that every excitation results in excimer formation, then $K(x) \gg (k_M + k'_M)$ and the excimer fluorescence quantum yield approaches its intrinsic value

$$\phi^*_E = \frac{k_E}{k_E + k'_E}. \tag{4}$$

As previously stated, by making the reasonable assumption that both mono and dipyrenyl probes dispersed in similar lipid environments exhibit the same limiting quantum yields, we can introduce these experimental parameters determined with the $py_{10}PC$ probes in the analysis of the $dipy_{10}PC$ data. Therefore, if we define the quantum yield ratios

$$r = \frac{\phi_E}{\phi_M} \quad r^* = \frac{\phi^*_E}{\phi^*_M} \tag{5}$$

then it follows from Eqs. 1 to 5 that $K$, the intramolecular excimer formation rate at atmospheric pressure, is given by

$$K = \frac{r}{r^*}\tau_M^{-1} \quad (6)$$

where $\tau_M = (k_M + k'_M)^{-1}$ is the excited state lifetime of the isolated $py_{10}PC$. Since the emission spectrum does not shift under the experimental conditions used, the monomer and excimer fluorescence intensities, $I_M$ and $I_E$, of the dipyrenyl probes are proportional to their respective quantum yields and may be conveniently used in their place. Likewise for the monopyrenyl probes, the relative fluorescence yields, defined as $J_M(x) = I_M(x)/x$ and $J_E(x) = I_E(x)/x$, are proportional to the absolute quantum yields, so that $\phi_M(x) = \alpha_M J_M(x)$, $\phi_E(x) = \alpha_E J_E(x)$, $\phi_M^* = \alpha_M J_M^*$, and $\phi_E^* = \alpha_E J_E^*$, where $\alpha_M$ and $\alpha_E$ are constants characteristic of the spectrofluorometer. The values of $J_M^*$ and $J_E^*$ are obtained from the analysis of monomer and excimer fluorescence yields as a function of $py_{10}PC$ molar fraction in the same lipid systems (Sassaroli et al., 1990).

The intramolecular excimer formation rate at pressure $P$, $K(p)$, is then given by:

$$K(p) = \frac{r(p)}{r^*(p)}\tau_M^{-1}(p), \quad (7)$$

where $r(p)$, $r^*(p)$, and $\tau_M(p)$ are the values of the parameters at pressure $P$; both $\tau_M$ and $r^*$ are expected to change with pressure because they include the nonradiative rates, $k'_M$ and $k'_E$, which are expected to be sensitive to pressure.

Therefore, the determination of $K(p)$ can, in principle, be accomplished only by measuring $r$, $r^*$, and $\tau_M$ as a function of pressure, which would require the very laborious application of the milling crowd model analysis, in which the mole fraction dependence of $py_{10}PC$ monomer and excimer fluorescence yields is obtained as a function of pressure and temperature (Eisinger et al., 1986; Sassaroli et al., 1990).

In practice, we have been able to avoid this by taking into account the following two considerations. First, in the absence of pressure-induced spectral shifts, $\tau_M(p)$ can be estimated from the monomeric fluorescence intensity at 1 bar, $I_M$, and at pressure $P$, $I_M(p)$, of $py_{10}PC$ dispersed in the MLV of interest at $x \approx 0.001$, a mole fraction low enough to preclude any excimer formation, and from the known value of $\tau_M$, the lifetime at atmospheric pressure at the same temperature

$$\tau_M(p) = \frac{I_M(p)}{I_M}\tau_M. \quad (8)$$

Second, from an empirical analysis of data previously obtained at atmospheric pressure (Vauhkonen et al., 1990), we have found a linear relationship between $J_M^*$ and $r^*$ in each of the lipid matrices investigated over a broad range of temperatures and even across phase transitions; representative data for DMPC and DOPC, together with the best-fit lines, are shown in Fig. 1. On this basis, we have assumed that such a linear correlation holds as a function of pressure as well, and we have derived the values of $r^*(p)$ according to the following equation

$$r^*(p) = \alpha\frac{I_M(p)}{I_M}J_M^*, \quad (9)$$

where $\alpha = dr^*/dJ_M^*$ is the slope of the lines in Fig. 1.

By adopting these two simplifications, $K(p)$ can be determined simply by measuring $I_M(p)$, the pressure-dependent monomeric fluorescence intensity of MLV labeled with $py_{10}PC$, from which the values of $\tau_M(p)$ and $r^*(p)$ are derived according to Eqs. 8 and 9 and $r(p)$, the pressure dependent excimer/monomer ratio in similar MLV labeled with $dipy_{10}PC$, according to the following equation

$$K(p) = \frac{r(p)}{r}\frac{r^*\tau_M}{r^*(p)\tau_M(p)}K = \frac{r(p)}{r}\frac{r^*I_M}{r^*(p)I_M(p)}K. \quad (10)$$

The atmospheric pressure values of $J_M^*$, $\tau_M$, and $K$ at the various temperatures used in the present work were taken from a published report (Vauhkonen et al., 1990); missing values were calculated by interpolation.

## EXPERIMENTAL RESULTS

As discussed in the previous section, the determination of $K(p)$ requires measuring both the $dipy_{10}PC$ excimer/

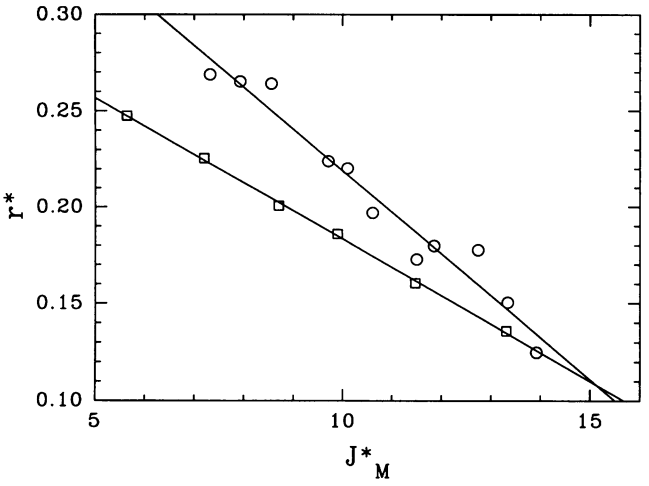


FIGURE 1 Limiting values of the excimer/monomer ratios, $r^*$, as a function of the monomer fluorescence yields, $J_M^*$, for $py_{10}PC$ in DMPC (○) and DOPC (□) MLV. The data were taken from a study in which the temperature dependence of the intermolecular excimer formation rate was determined according to the milling crowd model (Vauhkonen et al., 1990): each point in this plot represents the value obtained at a different temperature. Data for DPPC and POPC, not shown, display similar linear correlations.

monomer ratio, $r(p)$, and the monomer fluorescence intensity of $py_{10}PC$, $I_M(p)$, as a function of pressure in the membrane systems of interest.

Fig. 2 shows representative plots of $r(p)$ versus $P$ for $dipy_{10}PC$ in four model membrane systems at a few selected temperatures. As expected, the tighter lipid packing induced by the increasing hydrostatic pressure hinders the motions necessary for the two pyrene moieties to attain the proper separation and mutual orientation for excimer formation. The values of $r(p)$ are seen to monotonically decrease with pressure. Nevertheless, a qualitative difference can be noticed in the behavior of $r(p)$, depending on the chemical nature of the lipid matrix surrounding the $dipy_{10}PC$ probes. In the MLV composed of saturated phospholipid (DMPC and DPPC), $r(p)$ decreases linearly with increasing pressure until the onset of the liquid-crystalline to gel phase transition, at which point a sharp drop is observed followed by a more gradual, nonlinear decrease and leveling off in the gel phase. In the unsaturated lipid matrices (POPC and DOPC), on the other hand, the decrease in $r(p)$ appears to be nonlinear throughout the pressure and temperature ranges investigated, over most of which these MLV remain in the fluid phase. Furthermore, the liquid-crystalline to gel phase transition in POPC is marked by a much smaller drop in $r(p)$ as compared with the saturated lipids. As expected, no pressure-induced phase transition is detected in DOPC within the temperature and pressure ranges covered in this work.

From the midpoint of the sharp drop of $r(p)$, the value of the hydrostatic pressure $P_m$, at which the lipid matrix undergoes the pressure induced liquid-crystalline to gel phase transition, can be determined. Fig. 3 shows the temperature dependence of $P_m$ as determined by the intramolecular excimeric probe $dipy_{10}PC$ in these model systems. The slopes of the linear fits of $P_m$ versus $T$ yield the values of $dP_m/dT$ listed in Table 1; they are in good agreement with estimates from volumetric measurements, 43.5 atm $°C^{-1}$ for DPPC (Liu and Kay, 1977), from the pressure dependence of DPH polarization, 44.6

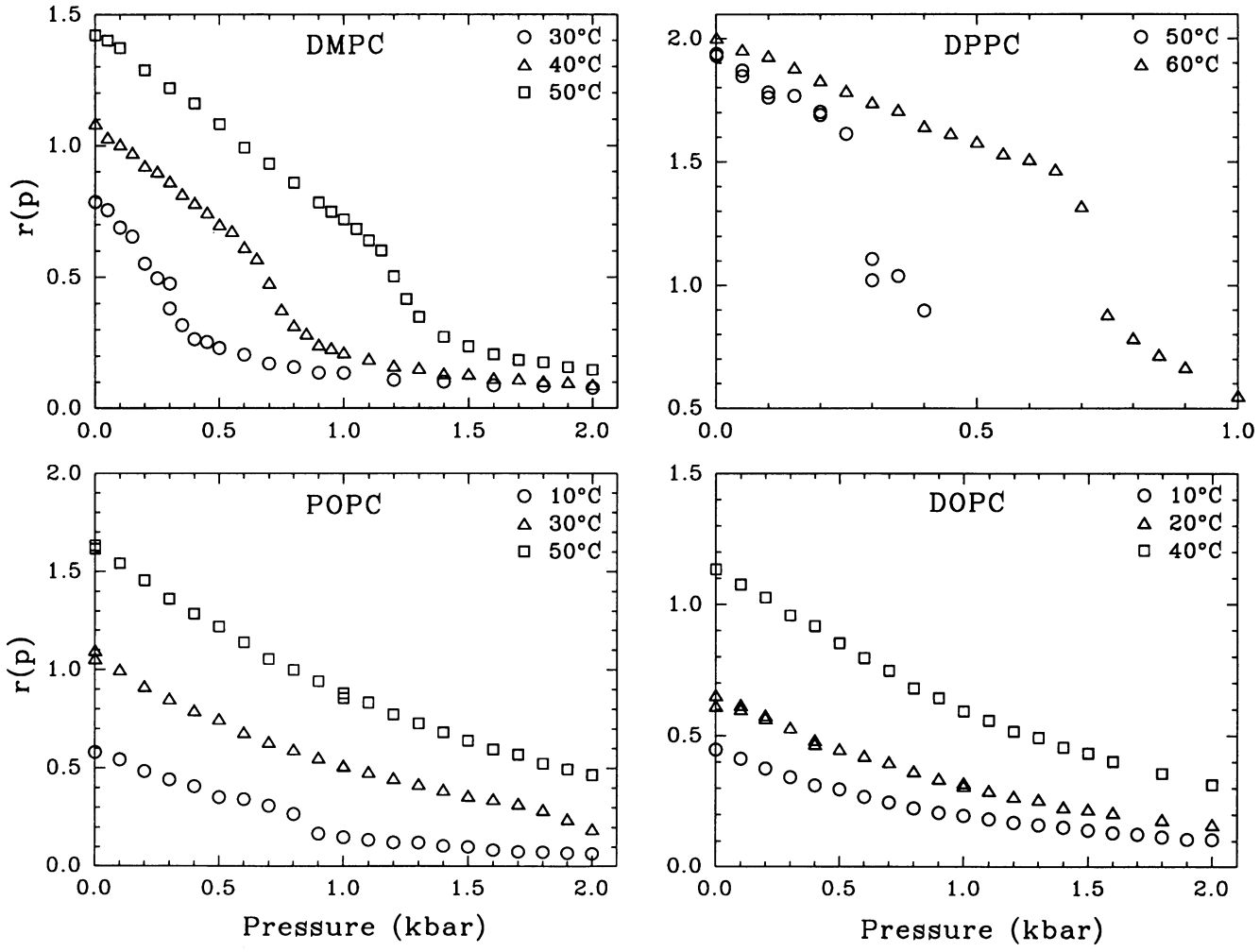


FIGURE 2 Pressure dependence of $r(p)$ for $dipy_{10}PC$ in MLV of DMPC, DPPC, POPC, and DOPC at a few selected temperatures. The sharp breaks in the DMPC and DPPC data correspond to the pressure-induced liquid-crystalline to gel phase transitions of the respective lipid matrices. In the case of POPC MLV, the phase transitions are signaled by much smaller drops in the values of $r(p)$, i.e., at $\approx$0.8 and 1.8 kbar for 10 and 30°C, respectively.

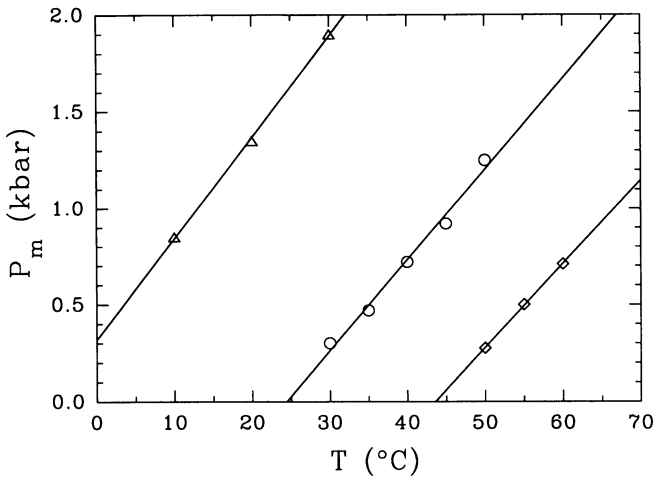


FIGURE 3 Temperature dependence of the phase transition pressure, $P_m$, for DMPC (○), DPPC (◇), and POPC (△). Values of $P_m$ were determined as the midpoints of the breaks in the plots of $r(p)$ versus $P$ shown in Fig. 2.

and 41.2 bar °C$^{-1}$ in DMPC and DPPC MLV, respectively (Chong and Weber, 1983), and from the pressure dependence of the excimer/monomer ratio for dipyrenylpropane in DMPC, 41.1 atm °C$^{-1}$ (Turley and Offen, 1985).

The atmospheric pressure values of $T_m$, the gel–liquid-crystalline phase transition temperature, obtained by extrapolating the linear fits to $P_m$ = 1 bar, are 24.4, 43.6, and −6°C for DMPC, DPPC, and POPC, respectively. They are also in fair agreement with accepted values (cf. Table 1 and references therein), the differences being due to uncertainties in our determination of $P_m$ and, possibly, to a small thermal gradient between the sample and the point at which the temperature is measured in our pressure vessel.

To translate the phenomenological intensity ratios, $r(p)$, into absolute intramolecular excimer formation rates, $K(p)$, according to Eq. 10, we measured the monomeric fluorescence intensity of $py_{10}PC$ at a probe/lipid mole fraction $x$ = 0.001 as a function of pressure and temperature and used it to calculate $\tau_M(p)$ and $r^*(p)$ according to Eqs. 8 and 9. In all model systems investigated (data not shown), $I_M(p)$ increases as a function of pressure; this is mainly due to a decrease in the rate of quenching by oxygen, which is most pronounced at the onset of the phase transition in DMPC and DPPC (Fischkoff and Vanderkooi, 1975).

In Fig. 4 representative semilogarithmic plots of the values of $K(p)$, calculated according to Eq. 10, versus pressure are shown for all the lipid MLV examined. The pressure-induced liquid-crystalline to gel phase transition remains clearly evident in the DMPC and DPPC data. The qualitative difference between the two lipid environments noticed in the plots of the raw $r(p)$ data in Fig. 2 is also preserved after conversion to $K(p)$, which eliminates any spurious effects due to pressure-induced changes in lifetimes. By transforming the empirical excimer/monomer fluorescence intensity ratios into absolute reaction rates, we are able to apply standard methods to the thermodynamic analysis of our data to obtain the activation parameters associated with intramolecular excimer formation. In particular, the apparent volume of activation, $V_a$, at temperature $T$ can be calculated according to the following equation,

$$2.303RT\left(\frac{\partial \log K(p)}{\partial P}\right)_T = -V_a, \qquad (12)$$

where $\partial \log K(p)/\partial P$ is the slope of the lines obtained by fitting the low-pressure, liquid-crystalline phase data in Fig. 4. The values of $V_a$ for DMPC MLV are plotted as a function of $T$ in Fig. 6 *a*, which shows that the activation volume for intramolecular excimer formation decreases monotonically with temperature. Owing to experimental difficulties related to failure of the sample cuvette cap on pressurization at temperatures above 60°C, we were able to complete measurements on DPPC MLV only at three temperatures, 50, 55, and 60°C, for which the values of $V_a$ are 23, 18.6, and 19.5 ml mol$^{-1}$, respectively.

The pronounced curvature in the pressure dependence of $K(p)$ in POPC and DOPC makes it impossible to derive a unique value of $V_a$ at each temperature. Using two exponentials, we were able to obtain very good fits to the data, as shown for a representative case by the solid line in Fig. 5, but the fitting parameters were highly correlated and thus were considered inaccurate. The data in the low- and high-pressure regions were then analyzed by use of linear fits of the semilogarithmic plots, shown by the straight lines in Fig. 5, and the estimated values of $V_a$ in the two pressure regions for both POPC and DOPC are shown in Fig. 6 *b* as a function of temperature.

To complete the thermodynamic description of the $dipy_{10}PC$ intramolecular excimer formation process in

**TABLE 1 Thermodynamic parameters of the liquid-crystalline to gel phase transitions in three host phospholipid MLV as revealed by the intramolecular excimeric $dipy_{10}PC$ probes**

| Host lipid | $dP_m/dT$ | $T_m$ | $\Delta H$ | $\Delta V$ (This work) | $\Delta V$ |
|---|---|---|---|---|---|
| | *bar °C$^{-1}$* | *°C* | *kcal mol$^{-1}$* | *ml mol$^{-1}$* | *ml mol$^{-1}$* |
| DMPC | 47.0 | 23.9* | 5.4* | 16.0 | 18.3§ |
| DPPC | 43.5 | 41.4* | 8.7* | 26.6 | 27.2§ |
| POPC | 52.5 | −5.0‡ | 8.0‡ | 23.8 | |

The second column lists the pressure to temperature equivalence values obtained from the linear fits of $P_m$ versus $T$ shown in Fig. 3. Values of the gel–liquid-crystalline phase transition temperature, $T_m$, and enthalpy, $\Delta H$, were taken from *Mabrey and Sturtevant (1976) and ‡DeKruyff et al. (1973). The values of $\Delta V$, the volume change at the phase transition, in the fifth column were calculated according to the Clausius-Clapeyron equation given by Eq. 14. For comparison, the experimental values of $\Delta V$ determined by density measurements are listed in the sixth column: §Nagle and Wilkinson (1978).

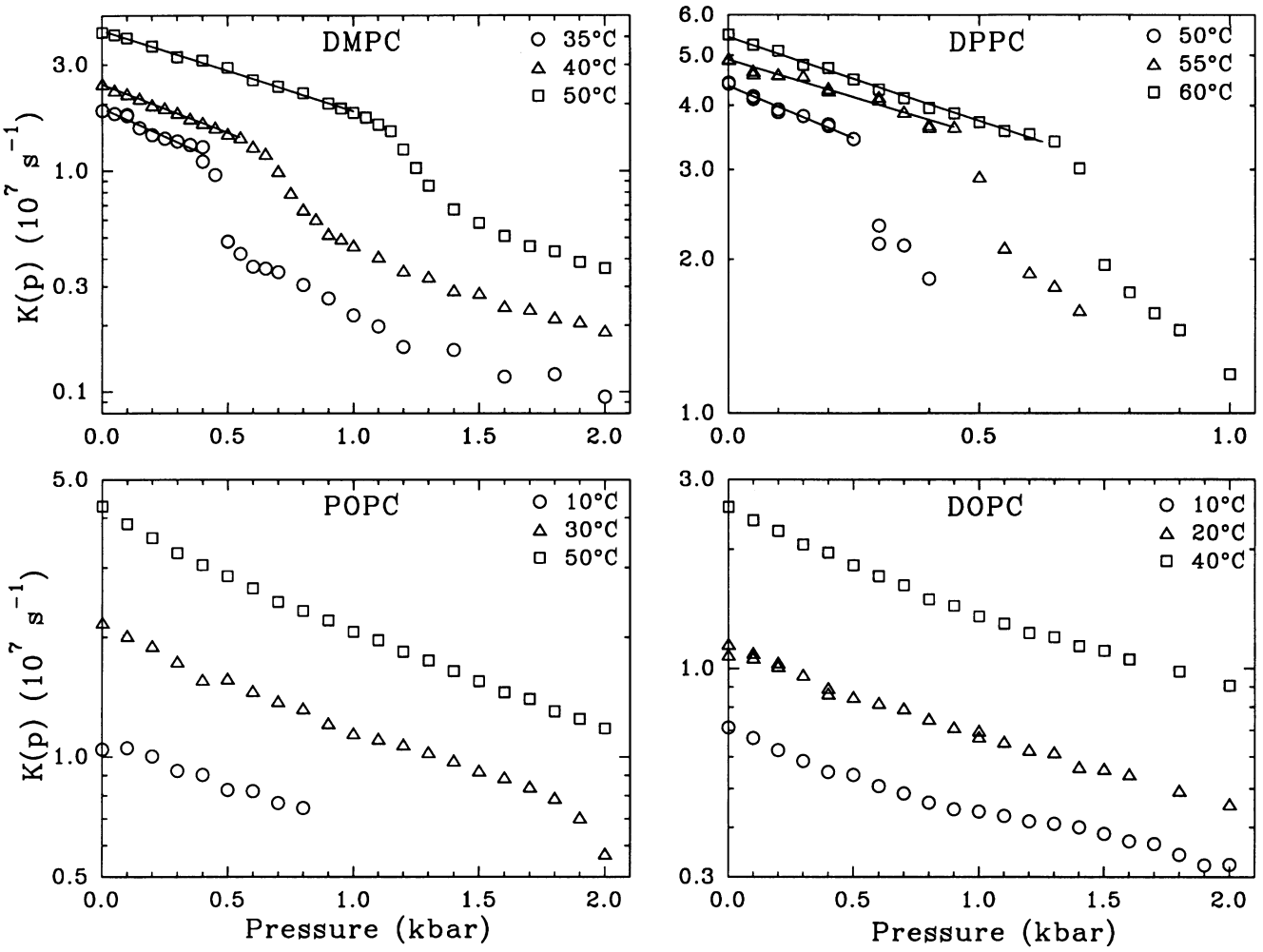


FIGURE 4 Pressure dependence of the intramolecular excimer formation rate, $K(p)$, for dipy$_{10}$PC in MLV of DMPC, DPPC, POPC, and DOPC at a few representative temperatures. Also shown are the best-fit lines to the liquid-crystalline phase data for DMPC and DPPC MLV. From their slopes, values of the volume of activation for intramolecular excimer formation, $V_a$, were derived (cf. Eq. 12). Note the curvature in the POPC and DOPC plots, which precludes the reduction of the data to a unique value of $V_a$.

the various MLV, we have also determined the temperature dependence of $K(p)$ at various pressures by analyzing the liquid-crystalline phase data in Fig. 4 in terms of the Eyring transition-state reaction theory, according to which the temperature dependence of $K(p)$ at constant pressure is given by

$$K(p) = \frac{kT}{h} \exp\left(\frac{\Delta S_a}{R}\right) \exp\left(-\frac{E_a}{RT}\right), \qquad (13)$$

where $h$ is Planck's constant, $k$ is Boltzmann constant, $T$ is the absolute temperature, and $\Delta S_a$ and $E_a$ are the apparent activation entropy and energy, respectively (Atkins, 1990). Linear fits of the data plotted as $\log(K(p)/T)$ versus $1/T$ yield values of $E_a$ from the slopes of the lines and of $\Delta S_a$ from the $1/T = 0$ intercepts. Representative plots for DMPC and DOPC MLV, together with the best-fit straight lines, are shown in Fig. 7 (note that the data shown are replotted from Fig. 4 and were not obtained by separate determination of $K(p)$ at constant pressure and variable temperature).

The values of $E_a$ and $\Delta S_a$ obtained from the fits in Fig. 7 are plotted as a function of pressure in Fig. 8 for DMPC and in Fig. 9 for POPC and DOPC. It is apparent that, apart from quantitative differences, qualitative differences exist between these lipid matrices in the response of both parameters to hydrostatic pressure. Whereas in DMPC $E_a$ increases with pressure, in the unsaturated phospholipid MLV it actually decreases. Similarly, although in DMPC $\Delta S_a$ is positive and increases with pressure, in POPC and DOPC it is negative at 1 bar and decreases as a function of pressure.

## DISCUSSION

Predictably, the application of high hydrostatic pressure inhibits excimer formation in all the phospholipid MLV examined. Yet our results also indicate that differences

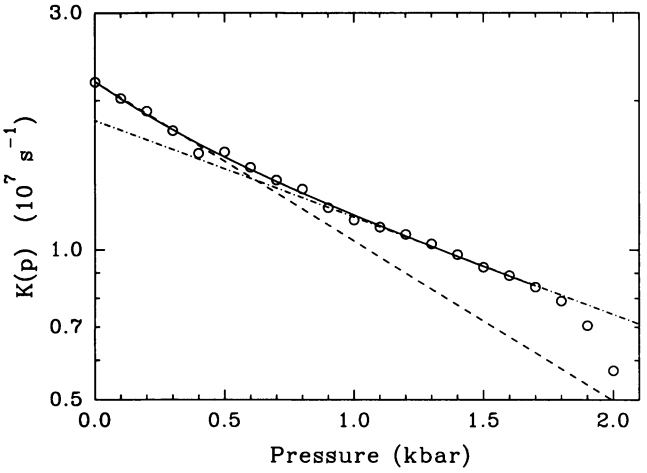


FIGURE 5 Representative example of the data analysis procedure used to obtain values of $V_a$ for the unsaturated lipid host MLV. The symbols represent the $K(p)$ values for dipy$_{10}$PC in POPC at 30°C. (——) Double exponential fit to the whole range of data in the liquid-crystalline phase; (---) the fit to the low pressure data; (-·-·-) the fit to the high pressure data.

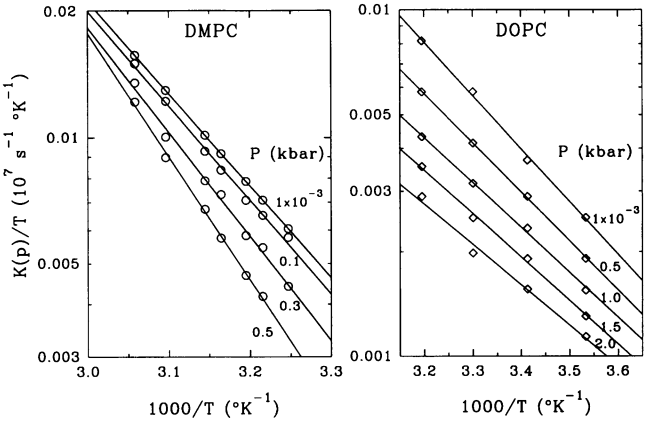


FIGURE 7 Representative Eyring plots of the intramolecular excimer formation rate, $K(p)$, as a function of inverse absolute temperature for dipy$_{10}$PC in DMPC and DOPC at a few selected pressures. Values of the activation energy, $E_a$, and entropy, $\Delta S_a$, as a function of pressure were derived from the slopes and intercepts of the lines, respectively (cf. Eq. 13). The plots for POPC MLV, not shown, were similar to those for DOPC (cf. Discussion and Fig. 9).

exist in the details of the pressure response of dipy$_{10}$PC probes in saturated and unsaturated lipid environments.

Before discussing the possible origin of these differences in greater depth, we provide additional evidence that the dipy$_{10}$PC probes are sensitive and reliable indicators of the thermodynamic state of their host bilayers. For this purpose, we apply the Clausius-Clapeyron equation

$$\frac{dP_m}{dT} = \frac{\Delta H}{T_m \Delta V}, \qquad (14)$$

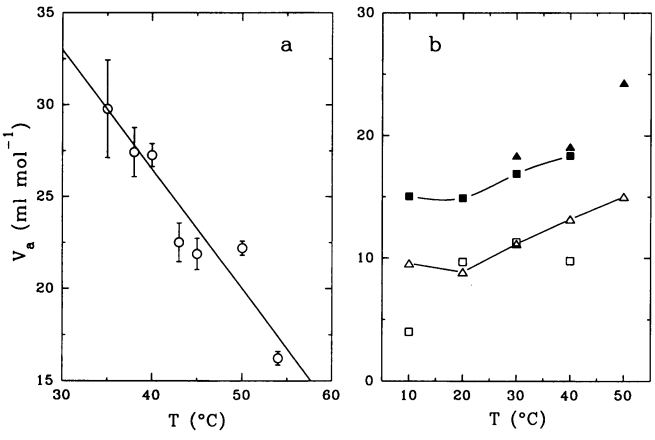


FIGURE 6 Temperature dependence of the volume of activation for dipy$_{10}$PC intramolecular excimer formation, $V_a$, in the various host MLV. (*a*) DMPC MLV: the slope of the best-fit line can be interpreted as the coefficient of thermal expansion of the DMPC lipid matrix (cf. Discussion). (*b*) data for POPC, (▲) low pressure and (△) high pressure range, and for DOPC, (■) low pressure and (□) high pressure range. The lines are included as an aid to eye and are not the result of a fit to any specific theoretical equation.

to calculate the volume change, $\Delta V$, at the phase transition using our values of $dP_m/dT$ and accepted values of $\Delta H$ and $T_m$. As shown in Table 1, the agreement of our estimates with those obtained from direct volume measurements is very good.

We now examine in more detail the various activation parameters to better understand the phospholipid-probe molecular interactions that affect the intramolecular excimeric reaction.

In the following discussion, we will adopt a simple model according to which excimer formation in dipy$_{10}$PC is rate limited by the rotational motion of one pyrene with respect to the other that is required to bring the initially separated excited and ground-state pyrene moieties into the proper spatial configuration for interaction to occur; all contributions from relative motions of the two pyrenes along the bilayer axis will be disregarded. Therefore, we will discuss the data assuming that the rate of intramolecular excimer formation is determined by the probability of occurrence of a rotation of sufficient amplitude within the excited state lifetime of the pyrene monomer. The various activation parameters will be related to this process within the framework of models developed to describe microscopic molecular motions and the "viscosity" or "free-volume" dependence of molecular diffusion and reaction rates in solution.

## Temperature dependence of the apparent activation volume for intramolecular excimer formation

### Saturated lipid MLV (DMPC and DPPC)

For both saturated lipid chain MLV, the analysis of the pressure dependence of $K(p)$ at each temperature ac-

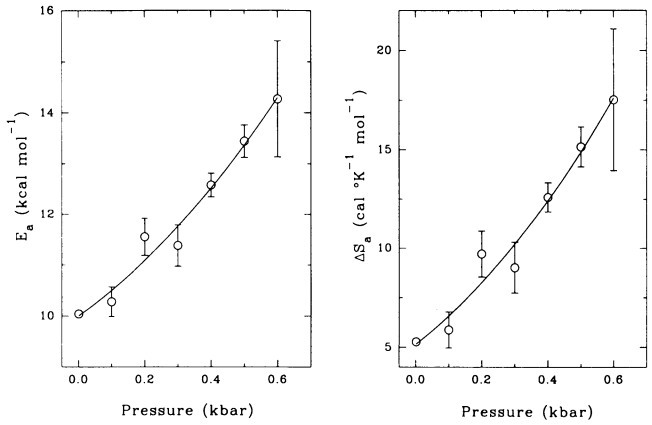


FIGURE 8 Pressure dependence of the apparent activation energy, $E_a$, and entropy, $\Delta S_a$, for dipy$_{10}$PC intramolecular excimer formation rate in DMPC MLV. The error bars represent the uncertainty of the values estimated from the standard deviations of the best-fit parameters for the Eyring plots in Fig. 7.

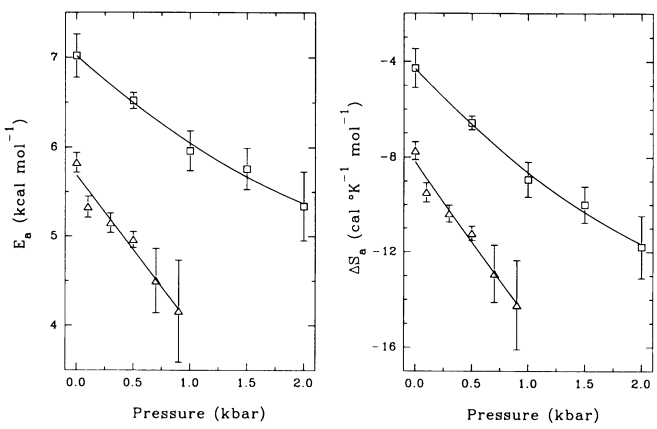


FIGURE 9 Pressure dependence of the apparent activation energy, $E_a$, and entropy, $\Delta S_a$, for dipy$_{10}$PC intramolecular excimer formation rate in (△) POPC and (□) DOPC MLV. The error bars represent the uncertainty of the values estimated from the standard deviations of the best-fit parameters for the Eyring plots in Fig. 7.

cording to Eq. 12 yields well-defined, single values of $V_a$ for the pressure range in which the lipid matrix is in the liquid-crystalline phase. In DMPC, for which data were collected over a sufficiently wide range of temperatures, $V_a$ decreases as a function of temperature as shown in Fig. 6 *a*. If we assume that the activated state in the intramolecular excimer reaction is attained when at least one of the two pyrene moieties can undergo unhindered rotation and that the volume of this activated state is temperature-independent and larger than both the ground state (in kinetic terms, not to be confused with the electronic ground or excited states of the pyrene molecules) and the excimeric state, then the decrease in the value of $V_a$ as a function of temperature must arise from an increase in the volume available to the ground state. This conclusion is consistent with the well-established thermal expansion of lipid bilayers. From density measurements, Nagle and Wilkinson (1978) concluded that the value of the thermal expansivity, $(\partial V/\partial T)_p$, for liquid-crystalline DMPC is $\sim$0.68 ml °C$^{-1}$ mol$^{-1}$ several degrees above $T_m$ and decreases to about half of that value at 50°C. Instead, as shown in Fig. 6 *a*, our data appear to be sufficiently well described by a constant value of $0.65 \pm 0.11$ ml °C$^{-1}$ mol$^{-1}$ between 35 and 54°C. Nevertheless, in view of the uncertainties and the limited number of our data points, this value is in quite reasonable agreement with the precise densitometric results, and it supports the validity of our assumptions.

In the case of DPPC MLV, as described in Experimental Results, measurements were successfully completed at only three temperatures, not sufficient for a meaningful estimation of the membrane thermal expansivity. Nevertheless, a few semiquantitative conclusions can be drawn. First, in DPPC, as in DMPC, $V_a$ appears to decrease with temperature, in agreement with Nagle's report of similar thermal expansivities for the saturated chain lecithins. Second, it was previously observed that, at the same reduced temperature, both inter- and intramolecular excimer formation rates were higher in DPPC than in DMPC, which was considered to be consistent with the chain length dependent increase of the volume per lipid acyl chain and with the free volume model of lipid diffusion (Vauhkonen et al., 1990). This conclusion is confirmed by the present study: at about 15°C above their respective $T_m$, $V_a$ is higher for DMPC ($\approx$27 ml mol$^{-1}$) than for DPPC ($\approx$19 ml mol$^{-1}$), whereas the atmospheric pressure value of $K(p)$ at the same temperatures is higher in DPPC than in DMPC.

Activation volumes of similar magnitude have been measured for intramolecular excimer formation of 1,3-di(1-pyrenyl)propane in various solvents (Hara and Yano, 1988). In that report, the authors were able to use the known pressure dependence of the solvent viscosity to separate the observed $V_a$ into two components: a small, negative intrinsic volume change for the intramolecular excimer formation and a large, positive activation volume due to the solvent viscous flow. Extrapolation of those results to our measurements would suggest that the contribution of the volume of activation of "microviscous" flow also dominates our values of $V_a$. However, we should point out that, despite the experimental efforts of several groups, determinations of the "microviscosity" of phospholipid bilayers based on similar extrapolations from data obtained in isotropic solutions have not yielded consistent results for reasons that may depend on the details of the molecular interactions between the probes and their surroundings. Moreover, even though hydrodynamic models, in which the lipid bilayer is assumed to be a continuum fluid with uniform viscosity, have been quite successful in describing the translational and rotational diffusion of large transmembrane proteins, their applicability to the Brownian

motion of lipids in lipid bilayers has been questioned (Saffman and Delbrück, 1975; Peters and Cherry, 1982; Vaz et al., 1985).

### Free volume model

In this section we will show how the free volume theory, initially developed to treat the problem of self-diffusion in fluid solutions (Cohen and Turnbull, 1959) and later adapted to two-dimensional diffusion in lipid bilayers (Galla et al., 1979; Müller and Galla, 1983; Vaz et al., 1985; King and Marsh, 1986), may be applied also to the analysis and interpretation of our results.

According to the original free volume model, molecular diffusion occurs as a result of molecules moving into voids of a size at least as large as some critical value, $v^*$, that are created by random redistribution of the free volume within the liquid. This theory, which was found to provide very good fits to the self-diffusion data for several liquids, should be applicable not only to translational diffusion but to any other process requiring large amplitude molecular motions within a dense medium, such as the rotation of the pyrene moieties within the lipid bilayer. Adapted to our specific case, this theory yields the following expression for the temperature and pressure dependence of the rate of intramolecular excimer formation

$$K = K_0 \exp\left(-\frac{v^*}{v_f}\right), \tag{15}$$

where $K_0$ is the value of the rate when $v_f \gg v^*$, i.e., in the gas phase, $v^*$ is the critical free volume, i.e., the minimum volume of the void required for free motion to occur, and $v_f$ is the temperature- and pressure-dependent average free volume per molecule, defined as

$$v_f = \bar{v} - v_0, \tag{16}$$

where $\bar{v}$ is the average volume of the molecule and $v_0$ is its van der Waals volume. In the case of translational diffusion, all volumes refer to the whole phospholipid molecule or, at least, to its acyl chains, whereas in the case of intramolecular excimer formation they may be related just to the pyrene moieties.

This simple formalism allows us to assign an intuitive physical meaning to the activation volume, $V_a$, as the size of the additional void volume needed to reach or exceed $v^*$ under conditions where the average ground-state free volume per molecule is $v_f$, or

$$V_a = v^* - v_f. \tag{17}$$

Upon substitution of Eq. 17 into Eq. 15, we obtain the following expression for the free-volume dependence of the intramolecular excimer formation rate

$$K = K_0 \exp\left(-\frac{v^*}{v^* - V_a}\right). \tag{18}$$

A consequence of this equation is that a large volume of activation is expected to correspond to a low excimer formation rate. This prediction is confirmed by the data plotted in Fig. 10, in which the values of the intramolecular excimer formation rate for $dipy_{10}PC$ in DMPC at atmospheric pressure for the various temperatures are plotted against their respective activation volumes. Also shown in Fig. 10 is the nonlinear least-squares fit to Eq. 18, which yields values of $K_0 = 22.1 \pm 2.4 \cdot 10^7\ s^{-1}$ and of $v^* = 49 \pm 3$ ml $mol^{-1}$, or $v^* \approx 80$ Å$^3$/molecule.

It is instructive to compare the experimental value of $v^*$ with a theoretical estimate obtained by subtracting the van der Waals volume, $v_0$, from the volume of revolution, $v_r$, of the pyrene molecule. On the basis of the crystal structure of pyrene (Robertson and White, 1947), by approximating the shape of the pyrene molecule to that of a prolate flat ellipsoid and assuming values of 5.5, 4.5, and 4.0 Å for its major and minor radii and its thickness, respectively, we obtain values of $v_0 \approx 310$ Å$^3$ and $v_r \approx 470$ Å$^3$. The resulting theoretical estimate of $v^* \approx 160$ Å$^3$ is twice the experimental value, which indicates that a partial rotation of one of the pyrene moieties with respect to the other may be sufficient for excimer formation.

The relationship between $K$ and $V_a$ also may be used to estimate the volume change sensed by the $dipy_{10}PC$ probes at the pressure-induced lipid phase transition: from Fig. 4 it can be seen that for DMPC at $T = 35$°C, $K$ drops from $\approx 1.0 \cdot 10^7\ s^{-1}$ just below $P_m$ to $\approx 0.3 \cdot 10^7\ s^{-1}$ above $P_m$, corresponding to $V_a$ values of 33.2 and 37.6 ml $mol^{-1}$, respectively, and a $\Delta V_a$ of +4.4 ml $mol^{-1}$ in going from the liquid-crystalline to the gel phase. By comparison, for DPPC at 55°C, $K \approx 4.0$ and $2.0 \cdot 10^7$

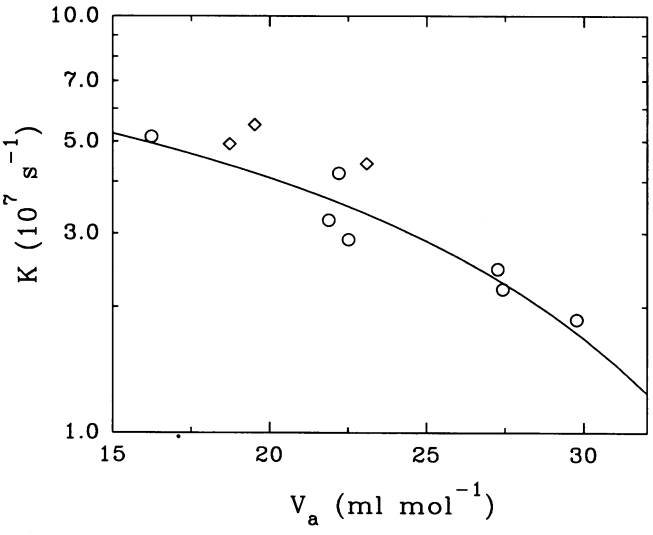


FIGURE 10 Semilogarithmic plot of the intramolecular excimer formation rate at atmospheric pressure, $K$, for $dipy_{10}PC$ in (○) DMPC as a function of the activation volume, $V_a$, calculated from its pressure dependence. Each point represents the value at a different temperature between 35 and 54°C. The line is the best fit to the data according to Eq. 18. Data for DPPC (◇) are also included to show the agreement with the DMPC values, although they were not used in the fit.

$s^{-1}$ below and above $P_m$, corresponding to values of 20.3 and 28.6 ml $mol^{-1}$ and a $\Delta V_a$ of +8.3 ml $mol^{-1}$. These values of $\Delta V_a$ suggest that the volume expansion at the gel–liquid-crystalline phase transition is larger in DPPC than in DMPC bilayers in qualitative agreement with the values of $\Delta V$ listed in Table 1.

### Unsaturated lipid MLV (POPC and DOPC)

Despite the uncertainties in the values of $V_a$ for the unsaturated lipids, the following observations can be made. First, $V_a$ for POPC and DOPC (Fig. 6 *b*) in both the low- and high-pressure regions are essentially identical over the whole temperature range examined in agreement with the fact that at atmospheric pressure, the values of $K$ for the two lipid matrices at each temperature are also very similar. Second, in contrast to the DMPC data, the values of $V_a$ in both pressure regions do not decrease with temperature but, on the contrary, appear to increase mildly above 20°C. If we follow the arguments presented in the previous section, then this observation leads us to conclude that the free volume within the unsaturated lipid matrix decreases with temperature. Third, if we apply Eq. 18 with the parameters obtained for DMPC, then from the atmospheric pressure values of $K$ at 10°C, $1.04 \cdot 10^7\ s^{-1}$ and $0.71 \cdot 10^7\ s^{-1}$ for POPC and DOPC, respectively, we should expect values of $V_a$ in excess of 30 ml $mol^{-1}$, at least twice as large as measured. Taken together, these last two observations indicate that the general free volume model proposed above for the saturated lipids cannot be directly extended to POPC and DOPC lipids and that specific interactions between the dipyrenyl probes and the unsaturated lipid chains must be taken into account to fully understand these results.

The finding that the semilogarithmic plots of $K(p)$ versus $P$ for unsaturated lipids (Fig. 4) are not linear, in contrast to those for the saturated lipids, also deserves some additional comments. At least three hypotheses may be proposed to account for this phenomenon and, possibly, for the unexpected temperature dependence of $V_a$. The first postulates that the coefficient of isothermal compressibility of the unsaturated lipid matrices decreases with pressure, in analogy with isotropic fluids (CRC Handbook of Chemistry and Physics, 1983). However, high-pressure fluorescence anisotropy studies using a series of anthroyloxy-fatty acid derivatives showed constant isothermal compressibility over this pressure range (Scarlata, 1991).

The second hypothesis emphasizes the dynamics of the system and postulates that in the unsaturated lipid bilayers the spontaneous volume fluctuations necessary for pyrene rotation and excimer formation occur with a frequency lower than the pyrene fluorescence decay rate. The curvature, then, originates from the pressure-dependent sampling of a distribution of local environments, each characterized by its specific value of $V_a$, that is heterogeneous on the time scale of the pyrene fluorescence lifetime ($\sim 10^{-7}$ s). As the pressure increases, the $dipy_{10}PC$ ground-state molecular configurations requiring the largest rotation to attain the proper orientation for excimer formation are progressively "frozen-out" and excimers form from those ground-state configurations that are already close to the optimal mutual orientation and thus require smaller free volumes of activation.

Finally, the third hypothesis invokes a pressure- (and temperature-) dependent change of the depth of the lipid *cis*-double bonds relative to that of the pyrene moieties due to increased ordering of the acyl chains. As a result, the dynamic properties or the compressibility of the pyrene environment may be modified, giving rise to effects similar to those described for the previous two hypotheses. This hypothesis is supported by the unsaturated bond occurring between carbons 9 and 10 in the oleic chains in almost exact coincidence with the point of attachment of the pyrenes at carbon 10. It thus appears plausible that the kinks introduced in the lipid acyl chains by the *cis*-double bonds might effectively hinder the rotational freedom of the pyrenyl moieties; this suggestion was advanced previously (Vauhkonen et al., 1990) to account for the observation that, at the same reduced temperature, the values of $f$, the $py_{10}PC$ lateral diffusion rate, and of $K$ are lower in POPC and DOPC than in DMPC and DPPC. Indeed, in preliminary experiments using MLV composed of 1-palmitoyl-2-petroselinoyl-*sn*-glycero-3-phosphatidylcholine (data not shown), in which the *cis*-double bond is between carbons 6 and 7, we have observed that $r(p)$ decreases linearly with pressure, in agreement with the saturated lipid data. Additional experiments, using a variety of unsaturated lipids and dipyrenyl probes with different acyl chain lengths, are needed to further substantiate these speculations.

## Pressure dependence of the activation energy and entropy for intramolecular excimer formation

The values of $E_a$ and $\Delta S_a$ for intramolecular excimer formation, calculated according to Eq. 13, are plotted as a function of pressure in Fig. 8 for DMPC and in Fig. 9 for POPC and DOPC. The difference between saturated and unsaturated lipids in their response to pressure, discussed above in reference to $V_a$, is confirmed by the pressure dependence of these thermodynamic parameters. In DMPC, raising the hydrostatic pressure from 1 bar to 0.5 kbar results in $E_a$ increasing by almost 4.0 kcal $mol^{-1}$, whereas $\Delta S_a$ increases from 5 to 15 cal $°K^{-1}$ $mol^{-1}$. For both unsaturated chain lipid MLV, on the other hand, $E_a$ decreases as a function of pressure, whereas $\Delta S_a$, already negative at atmospheric pressure, becomes progressively more negative. The atmospheric pressure value of $E_a$ in DMPC MLV, 10.0 kcal $mol^{-1}$, is very similar to

the values of 8.4 and 9.9 kcal $mol^{-1}$ for the intramolecular excimer formation of 1,3-di(1-pyrenyl)propane in DMPC MLV and sonicated unilamellar vesicles (Zachariasse et al., 1980; Melnick et al., 1981).

The positive pressure dependence of $E_a$ in DMPC MLV can be understood as arising from the higher energetic cost of molecular motion in the presence of the stronger intermolecular interactions induced by the increasing pressure. The increase of $\Delta S_a$ with pressure also can be accounted for by considering that the tighter packing of the lipid matrix should reduce the number of microstates sampled by each dipyrenyl probe in its thermodynamic ground state; this, in turn, will result in a larger gain in the number of accessible microstates, hence in a progressive increase in $\Delta S_a$, on reaching the activated state, in which we postulate that at least one of the two pyrenyl moieties has considerable rotational freedom.

On the other hand, the negative pressure dependence of $E_a$ and $\Delta S_a$ in POPC and DOPC MLV does not lend itself to a straightforward interpretation, and at least one of the specific effects of the *cis*-double bonds, mentioned in the preceding discussion of the non-linearity of the semilogarithmic plots of $K(p)$ versus $P$, must be invoked. It is noteworthy that a similar negative pressure dependence of $E_a$ and $\Delta S_a$ was observed in a study of the lateral fluidity in the membranes of intact erythrocytes using intermolecular excimeric probes (Eisinger and Scarlata, 1987).

## Linear free energy relationship for intramolecular excimer formation and structure of the $dipy_{10}PC$ excimer in phospholipid bilayers

From studies on a series of dipyrenylalkanes in a variety of alkane solvents, Zachariasse and Duveneck (1987) reported the existence of a linear free energy relationship correlating $\Delta H$ and $\Delta S$ for intramolecular excimer formation; they also showed that the data for different compounds could be divided into two groups, each fit by a straight line with slope $\beta = \partial\Delta S/\partial\Delta H$. As they discussed, the inverse of the slope of each of these lines is equivalent to the "isokinetic temperature" characteristic of the respective group, i.e., the temperature at which the excimer equilibrium constant for all compounds within the group is the same in all solvents examined. From this evidence, together with the finding that the two families of compounds also exhibit different excimer lifetimes, $\tau_E = (k_E + k'_E)^{-1}$, they concluded that intramolecular excimers may exist in two different structures: an asymmetric one, characterized by $\beta^{-1} = 304°K$ and $\tau_E \sim 70$ ns and exhibited, for example, by 1,16-di(1-pyrenyl)hexadecane, in which the two pyrene moieties are stacked in a parallel sandwich and shifted along their long axis by one aromatic carbon–carbon bond length as in the pyrene crystal (Robertson and White, 1947), and a less stable, symmetric one, with an isokinetic temperature $\beta^{-1} = 330°K$ and a $\tau_E \sim 150$ ns and exhibited by 1,3-di(2-pyrenyl)propane.

In Fig. 11, we present evidence that a similar linear relationship exists between the activation parameters for the intramolecular excimer formation of $dipy_{10}PC$ in the phospholipid matrices examined in this study. The atmospheric pressure values of $\Delta S_a$ versus $E_a$ are shown to be well fitted by a straight line (correlation coefficient $r > 0.999$) with a slope corresponding to an isokinetic temperature of $324 \pm 6$ °K. At this temperature, the apparent free energy of activation, $\Delta G_a$, and the rate of intramolecular excimer formation at atmospheric pressure, $K$, have the same values of 8.3 kcal $mol^{-1}$ and $\sim 4.0 \cdot 10^7$ $s^{-1}$, respectively, in all four lipid environments.

Although not obtained from measurements of the excited-state monomer/excimer equilibrium free energy, our value of isokinetic temperature is in satisfactory agreement with the higher of the two reported by Zachariasse and co-workers. This finding raises the unexpected possibility that the excimers formed by $dipy_{10}PC$ probes in phospholipid MLV may be constrained by their immediate surroundings to assume the less stable, symmetric structure exhibited by 1,3-di(2-pyrenyl)propane. This hypothesis will be tested by time-resolved fluorescence measurements of the excimer lifetime, $\tau_E$, of $dipy_{10}PC$ in MLV.

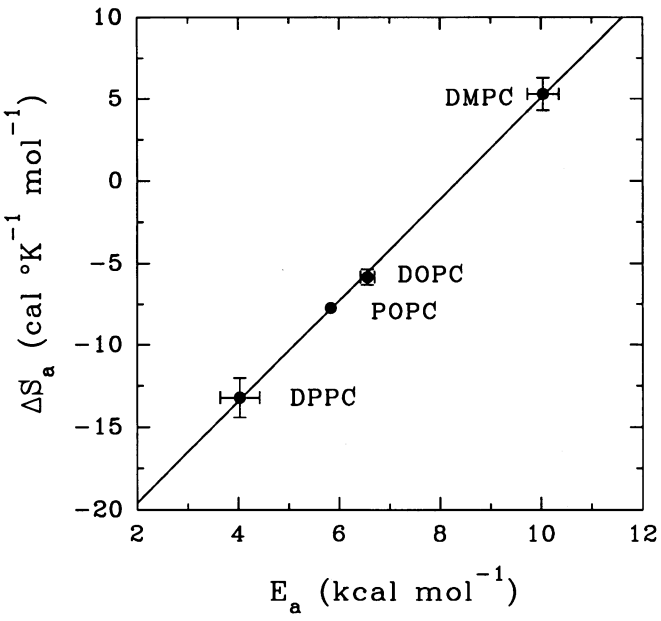


FIGURE 11 Plot of the apparent activation entropy, $\Delta S_a$, versus the apparent activation energy, $E_a$, for intramolecular excimer formation of $dipy_{10}PC$ at atmospheric pressure in the four MLV systems under study. The reciprocal of the slope of the fitted line is equal to the isokinetic temperature (cf. Discussion).

## CONCLUSIONS

We have shown how the pressure dependence of the intramolecular excimer formation rate for dipy$_{10}$PC in a variety of saturated and unsaturated phospholipid MLV can be determined from steady-state fluorescence measurements of their excimer/monomer ratios. The method is a straightforward extension of a previously developed model that makes use of experimental parameters of py$_{10}$PC probes in the same MLV. This study confirms that the dipy$_n$PC probes, used at very low concentration, are sensitive and precise indicators of the thermodynamic state of the host lipid membrane, as demonstrated by the agreement of our results with those obtained by techniques that use no extrinsic probes. We also have shown that, at least for saturated phospholipid membranes, a free-volume model can describe the pressure and temperature dependence of the intramolecular excimer formation rate.

Further work is needed to understand the differences in the pressure response of these probes in saturated and unsaturated lipid environments. Time-resolved fluorescence measurements also will be carried out to determine all the rate constants in the excimer reaction scheme and to assess the effect that the assumption of negligible excimer dissociation rate has on the values of $K$. A detailed characterization of their behavior in homogeneous model systems is expected to result in greater usefulness of the dipy$_n$PC probes in studies of biological membranes and, in particular, as tools in the determination of spatial variations of membrane fluidity by use of ratiometric fluorescence microscopy.

We thank Drs. Josef Eisinger and Istvan Sugar for many helpful discussions and for critically reading the manuscript.

This research was supported by National Institutes of Health grants 1R24-RR05272 and HL-21016 (M. Sassaroli) and GM-39924 (S. Scarlata).

*Received for publication 15 May 1992 and in final form 11 September 1992.*

## REFERENCES

Andrich, M. P., and J. M. Vanderkooi. 1977. Temperature dependence of 1,6-diphenyl-1,3,5-hexatriene fluorescence in phospholipid artificial membranes. *Biochemistry.* 15:1257–1261.

Atkins, P. W. 1990. Physical Chemistry. 4th ed. W. H. Freeman and Company, New York. 995 pp.

Bartlett, G. R. 1959. Phosphorous assay in column chromatography. *J. Biol. Chem.* 234:466–468.

Birks, J. B. 1970. Photophysics of Aromatic Molecules. John Wiley & Sons, Inc., New York. 301–371.

Chong, P. L.-G., and G. Weber. 1983. Pressure dependence of 1,6-diphenyl-1,3,5-hexatriene fluorescence in single-component phosphatidylcholine liposomes. *Biochemistry.* 22:5544–5550.

Cohen, M. H., and D. Turnbull. 1959. Molecular transport in liquids and glasses. *J. Chem. Phys.* 31:1164–1169.

CRC Handbook of Chemistry and Physics. 64th ed. 1983. R. C. Weast, editor. CRC Press, Inc. Boca Raton, FL.

Dale, R. E., L. A. Chen, and L. Brand. 1977. Rotational relaxation of the "microviscosity" probe diphenylhexatriene in paraffin oil and egg lecithin vesicles. *J. Biol. Chem.* 10:7500–7510.

Davenport, L., J. R. Knutson, and L. Brand. 1989. Fluorescence studies of membrane dynamics and heterogeneity. *Subcell. Biochem.* 14:145–188.

De Kruiff, B., R. A. Demel, A. J. Slotboom, L. L. M. Van Deenen, and A. F. Rosenthal. 1973. The effect of the polar headgroup on the lipid-cholesterol interaction: a monolayer and differential scanning calorimetry study. *Biochim. Biophys. Acta.* 307:1–19.

Eisinger, J., J. Flores, and W. P. Petersen. 1986. A milling crowd model for local and long-range obstructed diffusion: mobility of excimeric probes in the membrane of intact erythrocytes. *Biophys. J.* 49:987–1001.

Eisinger, J., and S. F. Scarlata. 1987. The lateral fluidity of erythrocyte membranes. Temperature and pressure dependence. *Biophys. Chem.* 28:273–281.

Fischkoff, S., and J. M. Vanderkooi. 1975. Oxygen diffusion in biological and artificial membranes determined by the fluorochrome pyrene. *J. Gen. Physiol.* 65:663–676.

Förster, Th., and K. Kasper. 1955. Ein Konzentrationsumschlag der Fluoreszenz des Pyrens. *Z. Elektrochem.* 59:977–980.

Galla, H.-J., and E. Sackmann. 1974. Lateral diffusion in the hydrophobic region of membranes: use of pyrene excimers as optical probes. *Biochim. Biophys. Acta.* 339:103–115.

Galla, H.-J., W. Hartmann, U. Theilen, and E. Sackmann. 1979. On two-dimensional passive random walk in lipid bilayers and fluid pathways in biomembranes. *J. Membr. Biol.* 48:215–236.

Hara, K., and H. Yano. 1988. High-pressure study on intramolecular excimer formation of 1,3-di-1-pyrenylpropane in various solvents. *J. Am. Chem. Soc.* 110:1911–1915.

Hresko, R. C., I. P. Sugar, Y. Barenholz, and T. E. Thompson. 1986. Lateral distribution of a pyrene-labeled phosphatidylcholine in phosphatidylcholine bilayers: fluorescence phase and modulation study. *Biochemistry.* 25:3813–3823.

King, M. D., and D. Marsh. 1986. Free volume model for lipid lateral diffusion coefficients. Assessment of the temperature dependence in phosphatidylcholine and phosphatidylethanolamine bilayers. *Biochim. Biophys. Acta.* 862:231–234.

Liu, N.-I., and R. L. Kay. 1977. Redetermination of the pressure dependence of the lipid bilayer phase transition. *Biochemistry.* 16:3484–3486.

Mabrey, S., and J. M. Sturtevant. 1976. Investigation of phase transitions of lipids and lipid mixtures by high sensitivity differential scanning calorimetry. *Proc. Natl. Acad. Sci. USA.* 73:3862–3866.

Melnick, R. L., H. C. Haspel, M. Goldenberg, L. M. Greenbaum, and S. Weinstein. 1981. Use of fluorescent probes that form intramolecular excimers to monitor structural changes in model and biological membranes. *Biophys. J.* 34:499–515.

Müller, H.-J., and H.-J. Galla. 1983. Pressure variation of the lateral diffusion in lipid bilayer membranes. *Biochim. Biophys. Acta.* 733:291–294.

Nagle, J. F., and D. A. Wilkinson. 1978. Lecithin bilayers. Density measurements and molecular interactions. *Biophys. J.* 23:159–175.

Paladini, A. A., and G. Weber. 1981. Absolute measurements of fluorescence polarization at high pressure. *Rev. Sci. Instrum.* 53:419–427.

Patel, K. M., J. D. Morrisett, and J. T. Sparrow. 1979. A convenient synthesis of phosphatidylcholines: acylation of *sn*-glycero-3-phosphatidylcholine with fatty acid anhydride and 4-pyrrolidinopyrene. *J. Lipid Res.* 20:674–677.

Peters, R., and R. J. Cherry. 1982. Lateral and rotational diffusion of bacteriorhodopsin in lipid bilayers: experimental test of the Saffman-Delbrück equations. *Proc. Natl. Acad. Sci. USA.* 79:4317–4321.

Robertson, J. M., and J. G. White. 1947. The crystal structure of pyrene. A quantitative x-ray investigation. *J. Chem. Soc. (Lond.).* 358–368.

Saffman, P. G., and M. Delbrück. 1975. Brownian motion in biological membranes. *Proc. Natl. Acad. Sci. USA.* 72:3111–3113.

Sassaroli, M., M. Vauhkonen, D. Perry, and J. Eisinger. 1990. Lateral diffusivity of lipid analogue excimeric probes in dimyristoylphosphatidylcholine bilayers. *Biophys. J.* 57:281–290.

Scarlata, S. F. 1991. Compression of lipid membranes as observed at varying membrane positions. *Biophys. J.* 60:334–340.

Turley, W. D., and H. W. Offen. 1985. Fluorescence detection of gel-gel phase transitions in DMPC vesicles at high pressures. *J. Phys. Chem.* 89:3962–3964.

Vauhkonen, M., M. Sassaroli, P. Somerharju, and J. Eisinger. 1990. Dipyrenylphosphatidylcholines as membrane fluidity probes. Relationship between intramolecular and intermolecular excimer formation rates. *Biophys. J.* 57:291–300.

Vaz, W. L. C., Z. I. Derzko, and K. Jacobson. 1982. Photobleaching measurements of the lateral diffusion of lipids and proteins in artificial phospholipid bilayer membranes. *Cell Surf. Rev.* 8:83–136.

Vaz, W. L. C., R. M. Clegg, and D. Hallmann. 1985. Translational diffusion of lipids in liquid crystalline phase phosphatidylcholine multibilayers. A comparison of experiment with theory. *Biochemistry.* 24:781–786.

Wu, E.-S., K. Jacobson, and D. Papahadjopoulos. 1977. Lateral diffusion in phospholipid multibilayers measured by fluorescence recovery after photobleaching. *Biochemistry.* 16:3936–3941.

Zachariasse, K. A., and G. Duveneck. 1987. Linear free energy relationships for excimers. *J. Am. Chem. Soc.* 109:3790–3792.

Zachariasse, K. A., W. Kühnle, and A. Weller. 1980. Intramolecular excimer fluorescence as a probe of fluidity changes and phase transitions in phosphatidylcholine bilayers. *Chem. Phys. Lett.* 73:6–11.